

On the Influence of Stratification and Continental Shelf and Slope Topography on the Dispersion of Subinertial Coastally Trapped Waves¹

DAVID C. CHAPMAN

Woods Hole Oceanographic Institution, Woods Hole, MA 02543

(Manuscript received 28 December 1982, in final form 3 June 1983)

ABSTRACT

The behavior of subinertial, coastally trapped free waves in a continuously stratified ocean is examined using a two-slope topography in which the continental shelf and slope are each represented by a single uniform slope. Surface-intensified stratification is assumed in which the squared buoyancy frequency profile is of the form $N^2 e^{\beta z}$, where N is the buoyancy frequency at the surface ($z = 0$) and β the vertical decay scale normalized by the deep-sea depth. The continental slope is typically assumed to be steeper than the shelf. Two qualitatively different types of dispersive behavior are distinguished. When $(N/f)a_2 > e^{\beta h/2}$, where f is the Coriolis parameter, a_2 the bottom slope of the continental slope, and h the shelf-break depth normalized by the deep-sea depth, then free waves may occur at any subinertial frequency, and each dispersion curve rises to f at some finite alongshore wavenumber (as in the case of baroclinic Kelvin waves). If $(N/f)a_2 < e^{\beta h/2}$, then all of the free-wave dispersion curves are limited to frequencies below some subinertial maximum, but are unlimited in wavenumber. This result is independent of the shelf width or shelf slope. Furthermore, for realistic shelf-break depths ($h \leq 0.2$), the result is only weakly dependent on β , and if $(N/f)a_2 \geq 3$ then the lowest-mode dispersion curve generally reaches f at a relatively small alongshore wavenumber (less than or equal to the wavenumber at which the corresponding flat-bottom, baroclinic-Kelvin-wave dispersion curve crosses f). Thus, because realistic values of $(N/f)a_2$ are typically of order 1 or greater, even seemingly weak stratification may be sufficient to cause the dispersion curves to go to f , and the stratification effects may be crucial for accurately modeling coastally trapped wave behavior, especially when short waves are important as in scattering or resonant interaction calculations.

1. Introduction

To date, the most complete theoretical treatment of subinertial, free, coastally trapped waves (CTW's) in a continuously stratified ocean with coastal topography has been presented by Huthnance (1978). He showed, among other things, that there is generally an infinite set of possible free-wave modes and that the frequency of each mode increases as the appropriate measure of stratification is increased. A rather striking consequence is that the *qualitative* behavior of any mode may be altered by changing the strength of the stratification. For example, a particular free wave mode in a weakly stratified ocean is usually limited to a finite subinertial frequency range, but it is unlimited in alongshore wavelength. Its group velocity typically decreases with decreasing wavelength, and it may allow energy propagation in either alongshore direction if the group velocity changes sign. These waves may be called frequency-limited modes. The same wave mode over the same topography in a strongly stratified ocean can occur at any subinertial frequency but is limited to relatively long wavelengths

(as in the case of baroclinic Kelvin waves). This wave typically has no zero group velocity and thus propagates phase and energy in the same direction. These waves may be called wavenumber-limited modes.² Using realistic ocean topography and stratification, Brink (1982) has presented examples of these behavioral differences; CTW's along the Oregon coast should be frequency-limited while those along the Peru coast should be wavenumber-limited.

Chapman and Hendershott (1982) have emphasized that this qualitative difference in behavior is also strongly dependent on the bottom topography [a result which is implicit in Huthnance's (1978) work]. Apparently, if the bottom topography is steep enough, then the waves can be wavenumber-limited even when the stratification is weak. The indication from

² At superinertial frequencies, these modes cannot be perfectly trapped because of the excitation of internal waves which transport energy away from the coast (except in the case of baroclinic Kelvin waves trapped at a vertical coastal wall). Instead, nearly trapped, superinertial counterparts to the perfectly trapped, subinertial modes can occur, an example of which has been given by Chapman (1982, Fig. 5) using an isolated step topography. Presumably, over complex coastal topography, there are similar nearly trapped, superinertial modes which represent leaky versions of baroclinic Kelvin-like waves, but the details have not been reported.

¹ Woods Hole Oceanographic Institution Contribution No. 5181.

both Huthnance (1978) and Chapman and Hendershott (1982) is that the steepest parts of the topography and the stratification there should primarily determine whether the free waves are frequency- or wavenumber-limited. A more quantitative understanding of this coupled effect of stratification and topography and the subsequent occurrence of each type of free wave is important, especially when considering problems like wave scattering or resonant interactions in which a detailed knowledge of the free-wave dispersion properties is necessary.

Considering the possible importance of even weak stratification, one may question the use of CTW models which completely ignore stratification effects. On the other hand, Clarke (1976) showed that when the offshore baroclinic length scale (a function of the stratification) is much less than the shelf-slope width, then stratification effects are negligible for long CTW's, and a barotropic model using Laplace's tidal equations (LTE) on an f -plane is appropriate. Huthnance (1978) generalized this result to shorter waves, but he also showed that CTW's with short spatial scales (either high alongshore wavenumber or high mode) resemble the bottom-trapped waves discussed by Rhines (1970) in which stratification is clearly important. This indicates that the accuracy of the barotropic approximation must diminish at high wavenumbers and high modes. Furthermore, barotropic models are expected to be most appropriate when the bottom topography is gently sloping and when the waves are frequency-limited even with stratification effects included (Chapman and Hendershott, 1982). Taken together these studies indicate the need for a better understanding of the general applicability of barotropic models.

This paper is an attempt to generalize on the relative influence of stratification, the continental shelf and the continental slope on CTW dispersion properties by considering free-wave solutions over the simple, yet fairly realistic, two-slope topography shown in Fig. 1. The constant bottom slopes a_1, a_2 represent the average slopes of the continental shelf and slope regions, respectively. A complete parameter study would be extremely lengthy, so several simplifications are made at the outset. Primary consideration is given to (i) the lowest-mode free wave which seems to be the most commonly observed mode, (ii) realistic topographies in which the continental slope is steeper than the shelf ($a_2 > a_1$), and (iii) smooth, exponential, surface-intensified stratification which can often approximate realistic stratification. Other situations are given limited attention.

The paper is organized in the following way. The equations governing the free-wave behavior are developed in Section 2. Some qualitative features of the predicted wave structures and dispersion curves are reviewed in Section 3. In Section 4, the result of a short-wave analysis due to Huthnance (1978, Section

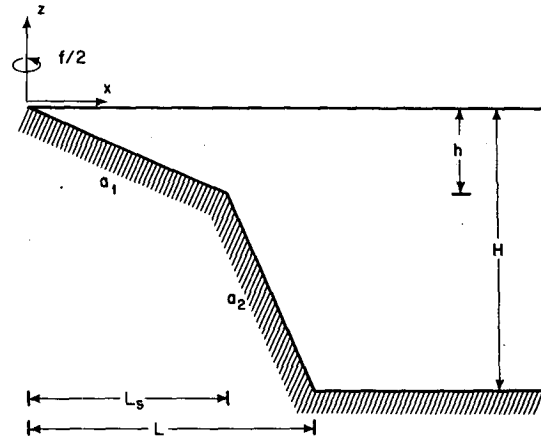


FIG. 1. A two-slope topography bordering a flat-bottom deep sea. Dimensional variables are shown. Slope a_1 represents the continental shelf while slope a_2 represents the continental slope.

7a) is used to distinguish between frequency- and wavenumber-limited waves. These results are combined in Section 5 with the near-inertial analysis of Huthnance (1978, Section 6c) to describe some features of wavenumber-limited waves. In Section 6, some long-wave phase speeds are calculated and compared to the equivalent barotropic model predictions. The implications of the results are discussed in Section 7 followed by a summary in Section 8.

2. Derivation of model equations

The fluid is assumed inviscid, incompressible, stratified, hydrostatic, Boussinesq and rotating at constant angular frequency $f/2$. All motions are assumed linear and traveling along the topography shown in Fig. 1 with frequency σ and alongshore wavenumber l (i.e., $\alpha e^{i\sigma t + il y}$). The equations of motion are

$$i\sigma u - fv = \frac{-1}{\rho_0} P_x, \tag{1a}$$

$$i\sigma v + fu = \frac{-il}{\rho_0} P, \tag{1b}$$

$$N_0^2 w = \frac{-i\sigma}{\rho_0} P_z, \tag{1c}$$

$$u_x + ilv + w_z = 0, \tag{1d}$$

where u, v, w are the offshore (x), alongshore (y) and vertical (z) velocities, respectively, P is the pressure perturbation, $N_0^2(z) \equiv -(g/\rho_0)\rho_{0z}$ the squared buoyancy frequency, and ρ_0 the undisturbed density. Subscripts (x, y, z) denote partial differentiation. Boundary conditions are

$$w = 0 \quad \text{at} \quad z = 0, \tag{2a}$$

$$w = 0 \quad \text{at} \quad x > L, \quad z = -H, \tag{2b}$$

$$w + D_x u = 0 \quad \text{at} \quad 0 < x < L, \quad z = -D(x), \tag{2c}$$

$$u, v, w, P \rightarrow 0 \text{ at } x \rightarrow \infty, \tag{2d}$$

where H is the deep-sea depth, L the total shelf-slope width, and D the bottom topography defined by

$$D(x) = \begin{cases} a_1x, & 0 < x < L_s, \\ a_2(x - L) + H, & L_s < x < L, \end{cases} \tag{2e}$$

in which L_s is the shelf width. The boundary conditions represent: (2a) a rigid lid, (2b,c) no flow through the solid bottom, and (2d) coastal trapping. The rigid lid filters out the surface Kelvin wave which is not of interest here.

The following scales are introduced in (1) and (2):

$$(x', y', L'_s, l') = (x/L, y/L, L_s/L, l/L),$$

$$(z', D', h') = (z/H, D/H, h/H),$$

$$(a_1^*, a_2^*) = (a_1L/H, a_2L/H),$$

$$Nn(z) = N_0(z),$$

where N is the maximum buoyancy frequency while $n(z)$ contains the z dependence. In scaled coordinates, the deep-sea depth and the total shelf-slope width are each unity. Combining (1) into a single equation for pressure and rewriting (2) in terms of pressure yields the following system of scaled equations (where the primes have been dropped for convenience):

$$\left(\frac{1}{n^2} P_z\right)_z + \frac{S^2}{1 - \omega^2} (P_{xx} - l^2 P) = 0, \tag{3a}$$

with boundary conditions

$$P_z = 0 \text{ at } z = 0, \tag{3b}$$

$$P_z = 0 \text{ at } x > 1, \quad z = -1, \tag{3c}$$

$$\omega P_z + D_x S^2 n^2 (1 - \omega^2)^{-1} (\omega P_x + l P) = 0$$

$$\text{at } 0 < x < 1, \quad z = -D(x), \tag{3d}$$

$$P \rightarrow 0 \text{ at } x \rightarrow \infty, \tag{3e}$$

where $S = (N/f)(H/L)$, $\omega = \sigma/f$ and

$$D(x) = \begin{cases} a_1^* x, & 0 < x < L_s, \\ a_2^* (x - 1) + 1, & L_s < x < 1. \end{cases} \tag{3f}$$

The stratification profile assumed here is surface-intensified with

$$n^2 = e^{\beta z}. \tag{3g}$$

The barotropic model equivalent to (3) is obtained by vertically integrating the continuity equation (1d), setting N_0 equal to zero in (1c)³ and eliminating the horizontal velocities. This yields (in scaled variables)

$$P_{xx} + \frac{D_x}{D} P_x + \left(\frac{D_x}{D} \frac{l}{\omega} - l^2\right) P = 0, \tag{4}$$

with boundary condition (3e) and D given by (3f).

3. Wave structure and dispersion curves

In this section some representative free-wave solutions of (3) and (4) are examined in order to illustrate the qualitative influence of stratification and topography. After specifying S , β and any two of a_1^* , a_2^* , h and L_s , Eq. (3) becomes a two-dimensional eigenvalue problem in either ω or l . Likewise, specification of any two of a_1^* , a_2^* , h and L_s , makes (4) a one-dimensional eigenvalue problem in either ω or l . Both (3) and (4) predict an infinite set of free-wave modes each of which travels with the coast on its right in the Northern Hemisphere. In general, the mode number corresponds to the number of zero crossings in the cross-shelf wave structure. For simplicity, only the lowest-mode wave (least cross-shelf structure) is considered in this section, and uniform stratification ($\beta = 0$) is assumed.

System (3) is solved here numerically by resonance iteration using a computer program generously provided by Dr. K. H. Brink which he has described elsewhere (Brink, 1982). A 17×25 vertically-stretched grid is used so that there are always 17 grid points in the vertical, regardless of the total depth. Eq. (4) is solved in a similar manner (using another of Dr. Brink's programs) with 25 grid spaces in x . These numerical schemes require a finite (non-zero) depth at the coast ($x = 0$), so an additional boundary condition is applied, namely,

$$u = 0 \text{ at } x = 0, \quad -d < z < 0.$$

The scaled depth d of this vertical coastal wall was taken in all cases to be $d = 0.001$. Its effect here is negligible. In addition, due to the limited spatial domain of the finite difference schemes used, (3e) is replaced by

$$u_x = 0 \text{ at } x = L_m.$$

Except for large choices of S in (3), the results are insensitive to L_m provided $L_m \geq 1.5$. To ensure that the grid spacing adequately resolves the coastal topography and still allows for some offshore decay, $1.5 \leq L_m \leq 2$ is used. Dispersion curves are calculated only up to $\omega \approx 0.8$, above which difficulties occur due to the spurious mode at $\omega = 1$ (Brink, 1982).

Fig. 2 shows alongshore velocity sections for two cases of lowest-mode waves obtained in the manner described above (the contour values shown are arbitrary). CTW's over a relatively steep shelf with moderately strong stratification (Fig. 2a; $S = 1$, $L_s = 0.4$, $h = 0.1$, $l = 0.01$) and over a wide shelf with weak stratification (Fig. 2b; $S = 0.222$, $L_s = 0.667$, $h = 0.1$, $l = 0.01$) each show features common to

³ This step implicitly assumes gentle topography so that the hydrostatic assumption is not violated. Otherwise, the left-hand side of (1c) would contain a term $(-\sigma^2 w)$ due to the vertical acceleration.

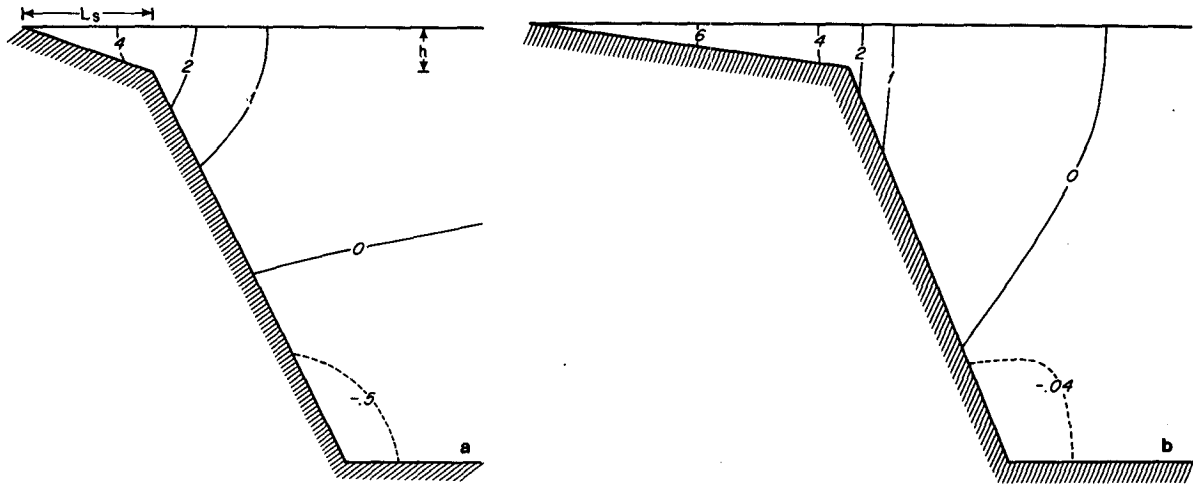


FIG. 2. Lowest-mode, alongshore velocity for (a) a relatively steep shelf with moderately strong stratification: $S = 1$, $L_s = 0.4$, $h = 0.1$, $l = 0.01$; and (b) a wide shelf with weak stratification: $S = 0.222$, $L_s = 0.667$, $h = 0.1$, $l = 0.01$. Stratification is uniform ($n^2 = 1$) and the contour values are arbitrary.

most first-mode CTW's (e.g., Huthnance, 1978; Brink, 1982). The flow is nearly barotropic over the shelf and upper slope. The largest velocities are concentrated near the coast and each mode-1 wave has one zero-crossing along the continental slope.

The velocity contours in Fig. 2 do suggest a difference in the behavior of the two waves, however. The nearly horizontal zero velocity contour in Fig. 2a suggests that this wave is like a baroclinic Kelvin wave, while the wave in Fig. 2b appears more barotropic. Such wave modal structures can be used to quantitatively distinguish CTW behavior (Brink, 1982), but dispersion curves offer a simpler way of showing the general effects of varying the scaled shelf width L_s and the stratification parameter S (Fig. 3). As mentioned above, Huthnance (1978) proved that increasing the stratification parameter S , while holding the other parameters fixed, must steepen the dispersion curves (i.e., increase the phase speed) as illustrated in Fig. 3a. Similarly, an increase in the shelf width L_s , while holding the other parameters fixed, steepens the mode-1 dispersion curve as shown in Fig. 3b. The relative increase in phase speed due to increasing S or L_s depends on the choice of the other parameters as well, but the qualitative effect is clear. The barotropic (LTE) prediction is shown in Fig. 3a to indicate that, even for small S , the barotropic model underestimates the frequency by an increasing amount as the alongshore wavenumber l increases, suggesting that the barotropic model is most appropriate for long waves. Fig. 3 also suggests that increasing S or L_s can change a frequency-limited dispersion curve to one which is wavenumber-limited (goes to f). With this in mind, the next section contains a quantitative examination of the ranges of pa-

rameters for which the dispersion curves are frequency- or wavenumber-limited.

4. Transition from frequency- to wavenumber-limited modes

The dispersion curves in Fig. 3a suggest that the transition from frequency-limited to wavenumber-limited free waves is a smooth function of S . That is to say that, for each topography, a critical stratification parameter S^c may be defined such that the mode-1 dispersion curve goes to f if $S > S^c$, but it does not reach f if $S < S^c$. In other words, S^c is that value of S for which the dispersion curve asymptotes to $f(\omega = 1)$ as the alongshore wavenumber becomes large. For example, in the special case of a finite-wedge shelf ($a_1^* = a_2^*$ or $h = L_s$) with uniform stratification ($\beta = 0$), $S^c = 1$ for each mode because the dispersion curve for each mode goes to f when $S > 1$ but does not reach f when $S < 1$ (Huthnance, 1978).

This idea may be generalized to other topographies by applying the large-wavenumber result of Huthnance (1978, Section 7a), i.e.,

$$\lim_{l \rightarrow \infty} \omega = S \max_z [nD_x],$$

where the maximum is taken over z and D_x is written as a function of z by using $z = -D(x)$. The critical stratification parameter is then defined by

$$1 = S^c \max_z [nD_x]. \quad (5)$$

Since (5) is independent of mode number, there is a single critical stratification parameter for each choice

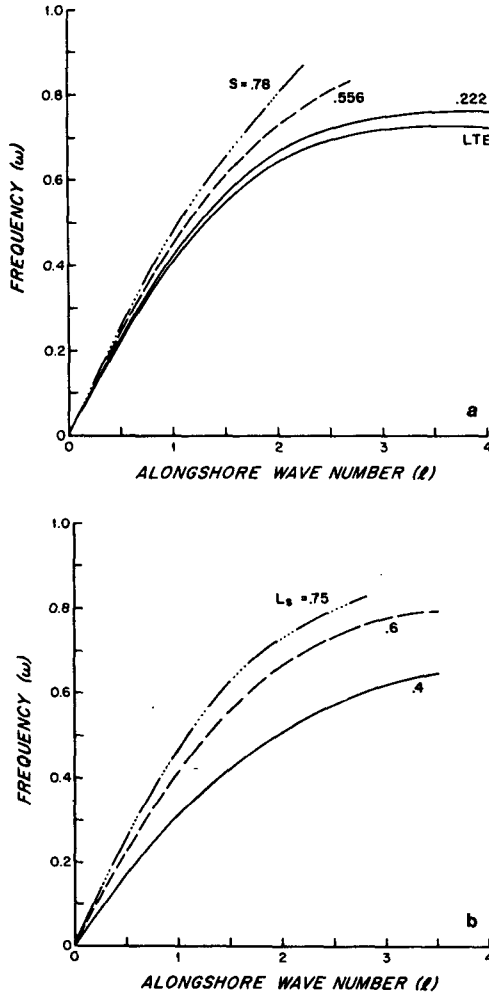


FIG. 3. Mode-1 dispersion curves for (a) different stratification parameters S with $L_s = 0.667$, $h = 0.1$, $n^2 = 1$; and for (b) different scaled shelf widths, L_s with $S = 0.4$, $h = 0.1$, $n^2 = 1$. The LTE prediction is also shown in (a) for comparison.

of topography $D(x)$ and stratification profile $n(z)$. Thus, if the dispersion curve for one mode goes to f , then all other dispersion curves go to f as well.

For the two-slope topography (3f) and the surface-intensified stratification (3g), Eq. (5) yields

$$S^c = \min(e^{\beta h/2}/a_2^*, 1/a_1^*). \tag{6}$$

This agrees with the result mentioned above for the uniformly-stratified finite-wedge shelf ($\beta = 0$, $a_1^* = a_2^* = 1$). Note that the large-wavenumber analysis of Huthnance (1978) is not strictly valid here because of the discontinuous bottom slope at the shelf break $x = L_s$. However, if (3f) is smoothed over some infinitesimal distance from the corner, then the changes produced in (6) are negligible. To illustrate the significance of (6), consider first the case of uniform stratification ($\beta = 0$). Since $Sa_2^* = (N/f)a_2$, then (6) is equivalent to stating that the boundary between

frequency-limited and wavenumber-limited dispersion regimes occurs at

$$\frac{N}{f} a_2 = 1 \quad \text{if } a_2 > a_1, \tag{7a}$$

$$\frac{N}{f} a_1 = 1 \quad \text{if } a_1 > a_2, \tag{7b}$$

where a_1, a_2 are the *unscaled* bottom slopes. In other words, for coastlines where the continental slope is steeper than the shelf ($a_2 > a_1$), if the quantity $(N/f)a_2 > 1$, then all dispersion curves go to f . If $(N/f)a_2 < 1$, then no dispersion curve reaches f . On the other hand, when the shelf is steeper than the slope ($a_1 > a_2$), if the quantity $(N/f)a_1 > 1$, then all dispersion curves go to f . If $(N/f)a_1 < 1$, then no dispersion curve reaches f . Note that these are *unscaled* bottom slopes so that the results (7a,b) are each independent of shelf width or shelf-break depth. Thus, with uniform stratification, the *steeper* bottom slope and the stratification completely determine whether or not the dispersion curves go to f .

The situation is not so simple with surface-intensified stratification ($\beta > 0$). However, if the discussion is limited to reasonably realistic topographies and stratifications (say $h \leq 0.2$, $a_2/a_1 \geq 5$, $\beta \leq 10$), then the boundary between frequency- and wavenumber-limited dispersion regimes occurs at

$$\frac{N}{f} a_2 = e^{\beta h/2}. \tag{8}$$

If $(N/f)a_2 > e^{\beta h/2}$, then all modes are wavenumber-limited. If $(N/f)a_2 < e^{\beta h/2}$, then all modes are frequency-limited. Thus, for the range of parameters considered, (8) shows that the continental slope and the stratification near the shelf break completely determine whether or not the dispersion curves go to f ; independent of the shelf slope or shelf width. Fig. 4 shows the wavenumber-limited and frequency-limited regimes as a function of β for various shelf-break depths h . The important point here is that the transition value of $(N/f)a_2$ changes at most by a factor of 2 even when the squared buoyancy frequency n^2 varies by more than three orders of magnitude from the surface to the bottom. This rather robust result suggests that weak, deep stratification has little effect on whether or not the dispersion curves go to f , and that (8) may provide a simple way of estimating the importance of stratification in real ocean situations. This will be discussed further in Section 7.

5. Near-inertial behavior

The results of the previous section define situations in which all dispersion curves go to f , thus suggesting the importance of stratification, but they do not show the relative magnitude of the stratification effects in those situations. After all, the dispersion curves could

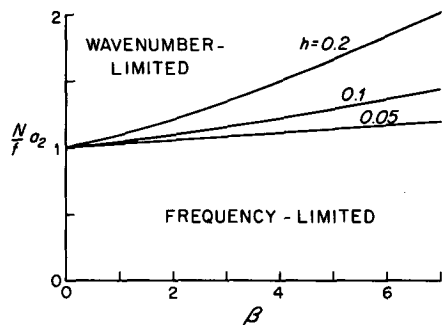


FIG. 4. Boundary between frequency- and wavenumber-limited dispersion regimes given by (8) with $h = 0.05, 0.1, 0.2$.

reach f at unrealistically large (albeit finite) alongshore wavenumbers, in which case it is unclear how important stratification is at the smaller and more realistic wavenumbers. Stratification, therefore, is expected to be most important for cases in which the dispersion curves are wavenumber-limited and reach f at relatively small alongshore wavenumbers. In this section, the relative effects of stratification on wavenumber-limited dispersion curves is examined by using the near-inertial analysis of Huthnance (1978, Section 6c) to determine the alongshore wavenumbers at which the dispersion curves reach f .

We consider a CTW with frequency slightly less than f , i.e., $\omega = 1 - \gamma$, where $\gamma \ll 1$, and let $P = [P_0(z) + \gamma P_1(x, z)]e^{-lx}$. To satisfy (3a) and (3d) at $O(\gamma)$,

$$P_1 = \frac{x}{lS^2} \frac{d}{dz} \left(\frac{1}{n^2} \frac{dP_0}{dz} \right), \tag{9a}$$

$$\frac{d}{dz} \left(\frac{e^{-2lx}}{n^2} \frac{dP_0}{dz} \right) + l^2 S^2 e^{-2lx} P_0 = 0, \tag{9b}$$

where $X(z)$ is defined by $z = -D(X)$. Boundary conditions for (9b) are obtained from (3b,c) as

$$\frac{dP_0}{dz} = 0 \quad \text{at } z = 0, -1. \tag{9c}$$

Eqs. (9b,c) form an eigenvalue problem in which, for given l, n^2 and $X(z)$, there is an infinite number of eigenvalues S_m . Each eigenvalue S_m corresponds to the stratification parameter necessary to make the mode m dispersion curve pass through $\omega = 1$ at the given l . Conversely, if S is specified, then the eigenvalues are l_m , and each l_m corresponds to the wavenumber at which the mode m dispersion curve reaches $\omega = 1$ for the chosen S .

To solve (9b,c), the inverse of the two-slope topography is determined from (3f) as

$$X(z) = \begin{cases} -z/a_1^*, & \text{at } -h < z < 0 \\ 1 - (z + 1)/a_2^*, & \text{at } -1 < z < -h, \end{cases} \tag{10}$$

and the stratification profile (3g) is again assumed.

Analytical solutions may be obtained when the stratification is uniform ($\beta = 0$; see the Appendix). Otherwise, (9b,c) is solved by applying a shooting method to a finite-difference representation of (9b). The boundary condition (9c) is assumed to be satisfied at $z = 0$. Then, for a chosen S , the value of l is varied until the integration of (9b) from $z = 0$ to $z = -1$ results in $dP_0/dz = 0$ at $z = -1$. This procedure, using 200 grid points, reproduces the uniform stratification results to within about 0.1%.

A complete characterization of the near-inertial behavior of CTW's is not attempted here. Instead, particular results are presented which illustrate properties of the wavenumber-limited modes directly pertaining to the importance of stratification over fairly realistic topographies. It is assumed here that stratification may be considered important if the scaled phase speed of a wavenumber-limited mode at the inertial frequency, $c_f = l^{-1}$, is greater than the phase speed c_K of the corresponding flat-bottom, baroclinic Kelvin wave. Fig. 5 shows the lowest-mode phase speed at the inertial frequency as a function of $(N/f)a_2$ with uniform stratification. The shelf slope is fixed at $a_1^* = 0.1$. The dotted curve corresponds to the minimum allowable bottom slope of the continental slope, $a_2^* = 1$. The dashed part of each constant- S curve is where $c_f < c_K = S/\pi$, while the solid part is where $c_f > c_K$. When S is small, $c_f \geq c_K$ at small $(N/f)a_2$. As S increases, $c_f \approx c_K$ over the entire range of $(N/f)a_2$. More quantitatively, if $S \leq 3$, then $c_f \geq 0.9 c_K$ when $(N/f)a_2 \geq 3$. If $S \geq 3$ (not shown), $c_f \geq 0.9 c_K$ for all $(N/f)a_2$. Almost identical quantitative results are obtained for other shelf slopes, 0.05

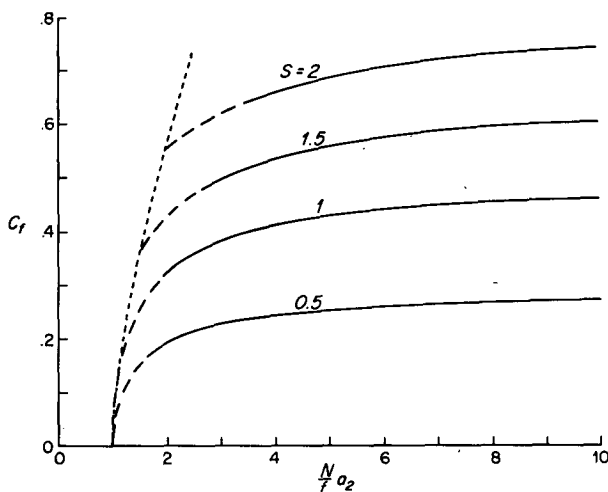


FIG. 5. Scaled, mode-1 phase speed at the inertial frequency, $c_f = l^{-1}$, versus $(N/f)a_2$ with uniform stratification ($\beta = 0$) and shelf slope $a_1^* = 0.1$. The dotted curve corresponds to $a_2^* = 1$. The dashed part of each curve is where c_f is less than the phase speed of the lowest-mode, flat-bottom, baroclinic Kelvin wave, $c_K = S/\pi$. The solid part is where $c_f > c_K$.

$\leq a_1^* \leq 0.3$. With surface-intensified stratification ($\beta > 0$), the qualitative features of Fig. 5 are unchanged, but as β increases, the phase speeds decrease due to the overall decrease in stratification. Thus, the mode-1 dispersion curve may reach f at relatively small wavenumbers even when S is fairly small, and $(N/f)a_2$ need not be much larger than the boundary value given by (8) for stratification to be important at fairly small wavenumbers.

The effects of varying the shelf-break depth are shown in Fig. 6 where the scaled, mode-1, phase speed at the inertial frequency c_f is plotted versus the scaled shelf-break depth h with uniform stratification ($\beta = 0$) and a vertical continental slope ($L_s = 1$ or $a_2^* = \infty$). When $h = 0$, the phase speed equals that of the flat-bottom, baroclinic Kelvin wave c_K . As h increases slightly from zero, the phase speed c_f increases in response to the gently sloping, shallow shelf. For large S , the phase speed always remains greater than or equal to c_K suggesting that stratification effects are important at all shelf-break depths. For small S , the phase speed decreases slowly toward $c_f = 0$ as $h \rightarrow 1$. The decrease toward zero represents the dispersion curve reaching f at ever larger alongshore wavenumbers. Thus, when S is small, stratification effects are expected to be important only if the shelf-break depth is a small fraction of the deep-sea depth. In effect, the weak stratification ($S < 1$) must be "felt" over a relatively large portion of the bottom topography to influence strongly the near-inertial behavior. This idea is further exemplified in Fig. 7 where the mode-1 phase speed at the inertial frequency is plotted versus h for surface-intensified stratification $\beta = 0, 2, 5$ and $S = L_s = 1$. As β increases, c_f remains larger than c_K over a smaller range of h . Once again the influence of stratification is apparently dictated by the portion of topography over which the stratification appears strong. Note, however, that in both

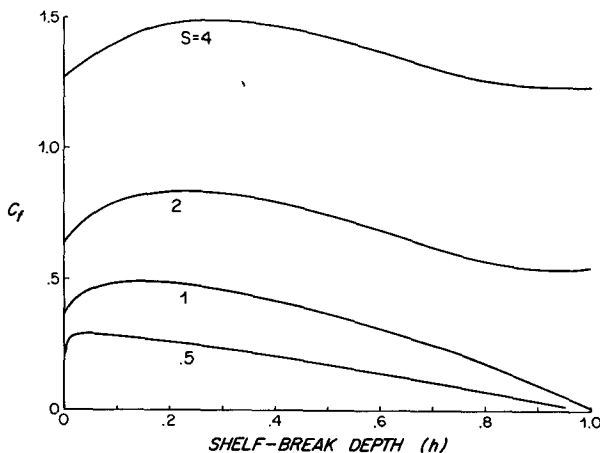


FIG. 6. Scaled, mode-1 phase speed at the inertial frequency c_f versus shelf-break depth h for several uniform stratifications ($n^2 = 1$) and a vertical continental slope ($L_s = 1$).

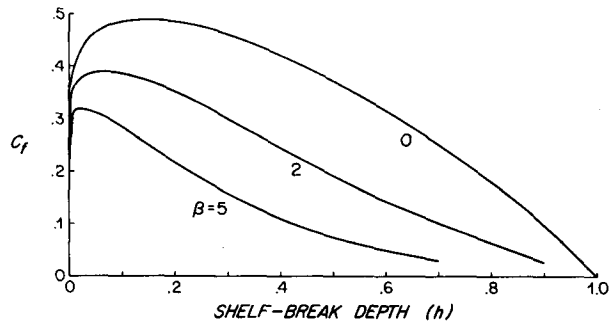


FIG. 7. As in Fig. 6 but for surface-intensified stratification $\beta = 0, 2, 5$ and $S = L_s = 1$.

Figs. 6 and 7 the phase speed at the inertial frequency is always larger than the baroclinic-Kelvin-wave phase speed for realistic shelf-break depths ($h < 0.2$). Although not shown here, this result also holds true for modes 2 and 3 and for continental slopes as gentle as $a_2^* = 2$. Thus, for realistic shelf-break depths, the dispersion curves again reach f at relatively small wavenumbers even when S is fairly small.

The effects of varying either the total shelf-slope width L or the latitude (f , essentially) are shown in Fig. 8. The product $c_f S^{-1}$ has been plotted (to remove the dependence of c_f on f and L) versus S^{-1} for mode 1 using several continental slopes with uniform stratification and fixed shelf slope $a_1^* = 0.1$. As $S^{-1} \rightarrow 0$, the mode-1 wave approaches a flat-bottom, baroclinic Kelvin wave for all topographies. As S^{-1} increases slightly from zero, the phase speed increases whenever $a_2^* > a_1^*$ (even the $a_2^* = 1.1$ curve increases slightly before decreasing), and decreases whenever $a_1^* > a_2^*$ (not shown) in agreement with Romea (1982).⁴ (This holds true for modes 2 and 3 as well.) As S^{-1} increases further, the dispersion curve reaches f at ever larger wavenumbers until the phase speed at the inertial frequency vanishes. This occurs at larger S^{-1} for larger a_2^* indicating that stratification is relatively more important when the continental slope is steep. When $a_2^* = \infty$, the dispersion curve goes to f at relatively small wavenumbers regardless of the latitude or shelf-slope width. Note that a_2^* need not be terribly large for c_f to be greater than c_K when S is fairly small. Thus, a small stratification parameter S does not guarantee that stratification effects are negligible.

6. Long-wave phase speed

In this section, long-wave phase speeds are calculated using the two-slope topography and compared

⁴ It is interesting to note that Romea (1982) found that if $a_1^* = a_2^*$, then increasing S^{-1} slightly above zero had no effect on the phase speed. However, for this case $c_f S^{-1} = (1 - S^{-2})^{1/2} / m\pi$ (Huthnance, 1978) and the change in phase speed appears as a second-order correction in S^{-1} whereas Romea (1982) only considered first-order corrections in S^{-1} .

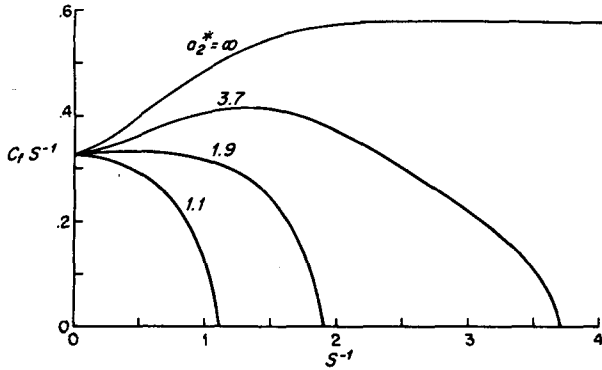


FIG. 8. Scaled, mode-1 phase speed at the inertial frequency (independent of f) $c_l S^{-1}$ versus inverse stratification parameter S^{-1} (latitude or shelf-slope width) with $a_1^* = 0.1$, $\beta = 0$ and $a_2^* = 1.1, 1.9, 3.7, \infty$.

with their barotropic counterparts to investigate the applicability of barotropic models. In the long-wave limit, the wave frequency σ and wavenumber l each approach zero, but the phase speed $c = \sigma/l$ remains finite. Thus (3) becomes

$$\left(\frac{1}{n^2} P_z\right)_z + S^2 P_{xx} = 0, \tag{11a}$$

with boundary conditions

$$P_z = 0 \text{ at } z = 0, \tag{11b}$$

$$P_z = 0 \text{ at } x > 1, z = -1, \tag{11c}$$

$$P_z + D_x S^2 n^2 (P_x + c^{-1} P) = 0$$

at

$$0 < x < 1, z = -D(x), \tag{11d}$$

$$P \rightarrow 0 \text{ at } x \rightarrow \infty, \tag{11e}$$

and $D(x)$ given by (3f). The barotropic model (LTE) equivalent to (11) is

$$P_{xx} + \frac{D_x}{D} P_x + \frac{D_x}{D} \frac{1}{c} P = 0. \tag{12}$$

Eqs. (11) and (12) are eigenvalue problems in c and are solved in the manner outlined for (3) and (4) in Section 3.

The general relationship between (12) and (11) has been investigated extensively by Clarke (1976), so a detailed treatment is not presented here. The results included here are merely intended to elucidate some features of long-wave behavior over the two-slope topography. Only first-mode waves are considered because higher modes seem to be more sensitive to the location of grid points in the numerical schemes. Fig. 9 shows contours of c calculated from (11) with $a_1^* = 0.1$ and uniform stratification ($\beta = 0$). The contours were interpolated from calculations of c at L_s intervals of 0.1 and S intervals of 0.25. As shown by Clarke (1976), the phase speed increases as the stratification

parameter increases. For narrow shelves ($L_s \rightarrow 0$), the phase speed depends primarily on S , but for wide shelves ($L_s \rightarrow 1$), the phase speed changes only slightly with S . Conversely, when S is small, the phase speed depends primarily on the shelf width, but for large S the phase speed is much less dependent on the shelf width.

The long-wave phase speeds of Fig. 9 are compared in Fig. 10 to the corresponding long-wave phase speeds predicted by the barotropic model [obtained using (12) with $a_1^* = 0.1$]. Because the barotropic model always underestimates the phase speed, the contours show the increase of long-wave phase speed over the barotropic predictions. The agreement is clearly better for small values of S regardless of L_s . The agreement also improves as the scaled shelf width L_s increases with S fixed suggesting that the shelf width is an important horizontal length scale in addition to the larger shelf-slope width L . Further, for $L_s \geq 0.2$, the contours roughly correspond to lines of $S \propto L_s$ which are the same as lines of constant $[(NH/f)/\text{unscaled shelf width}]$. This suggests that for $L_s \geq 0.2$, the ratio of the offshore baroclinic length scale (NH/f) to the *unscaled* shelf width primarily determines the percent error resulting from ignoring stratification effects. It is also interesting to note that the long-wave agreement may be good even in cases where the dispersion curves ultimately go to f (i.e., at large L_s).

Other choices of shelf slope ($0.05 \leq a_1^* \leq 0.2$) produce only slight quantitative changes in the above results. Surface-intensified stratification ($\beta > 0$) reduces the long-wave phase speed at each (S, L_s) location, thus improving the agreement between LTE and the stratified model. However, the qualitative

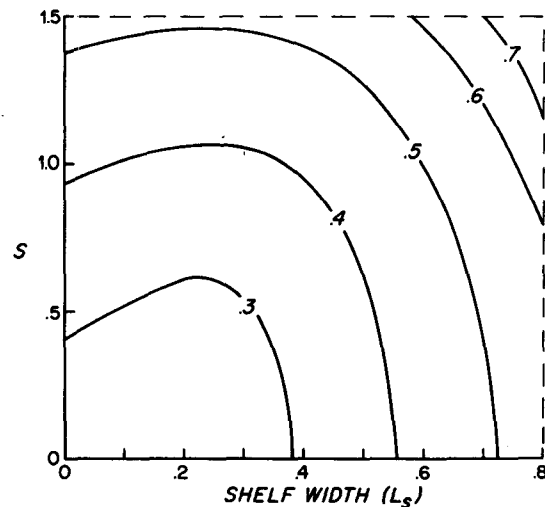


FIG. 9. Contours of dimensionless, mode-1, long-wave phase speed c on the (L_s, S) plane with $a_1^* = 0.1$ and uniform stratification ($n^2 = 1$).

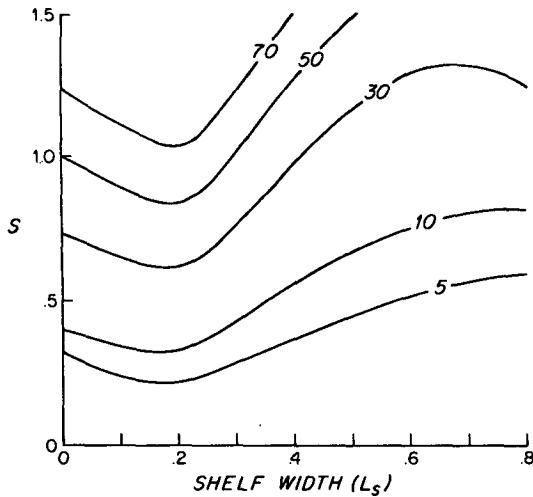


FIG. 10. Contours of the percent increase of c from Fig. 9 over the equivalent LTE prediction of long-wave phase speed; $a_1^* = 0.1$, $\beta = 0$.

result that the *unscaled* shelf width is an important horizontal length scale remains unchanged.

7. Discussion

With the increased availability of computer programs which numerically solve (3), it is probably fair to say that the details of CTW dispersion and modal structure for real ocean situations are best obtained by solving particular cases individually. However, some of the above results have implications beyond the simple topography considered here, and taken together they present a qualitative picture of CTW dispersion in a continuously stratified ocean with arbitrary topography.

A typical dispersion curve for any stratification and topography begins at the origin ($\sigma = l = 0$) with its slope (long-wave phase speed) greater than that of a barotropic model over the same topography. Present results suggest that the magnitude of the difference depends primarily on the ratio of the offshore baroclinic length scale to the unscaled shelf width. Clarke (1976) proved that the barotropic model represents the limit of the baroclinic length scale being much less than the total shelf-slope width, whereas the present calculations suggest that the *shelf* width may often

be more important than the larger shelf-slope width. This can be seen in Fig. 10 where the disagreement is substantial at small L_s , even for fairly small S (large L). If the total shelf-slope width L were the dominant horizontal length scale, then the percent-difference lines in Fig. 10 would be more nearly horizontal.

As the wavenumber increases, each dispersion curve rises to higher frequencies until it either reaches a frequency maximum or goes to f . According to (8), this transition occurs when $(N/f)a_2 \approx 1$ for realistic shelf-break depths. If $(N/f)a_2 \geq 1$, then all the dispersion curves go to f . If $(N/f)a_2 \leq 1$, then all the dispersion curves reach a subinertial frequency maximum. This result is independent of shelf slope or shelf width. Furthermore, Fig. 5 shows that if $(N/f)a_2 \geq 3$, then the mode-1 dispersion curve reaches f at a fairly small wavenumber (equal to or less than the l where the corresponding dispersion curve for the flatbottom, baroclinic Kelvin wave crosses f), and stratification effects are expected to be important. This is seen as a conservative estimate by noting that the dispersion curves in Fig. 3a correspond to $(N/f)a_2 = 0, 0.6, 1.5, 2.1$. Thus, even seemingly weak stratification should not be ignored *a priori* because it may still be sufficient to cause the dispersion curves to go to f at relatively small wavenumbers. For example, at midlatitudes ($f \approx 0.04$ cph) a continental slope with $a_2 = 0.03$ requires a surface buoyancy frequency of only $N \geq 4$ cph to make $(N/f)a_2 = 3$; independent of the magnitude of S . In fact, if the topography is steep enough, i.e., $a_2 \rightarrow \infty$, then all dispersion curves go to f for any stratification. This is presumably the case encountered with the step shelf (Chapman and Hendershott, 1982).

Further support for these conclusions may be obtained by applying the analysis of Sections 4 and 5 to an exponential topography similar to that which has been used to model real topography (e.g., Buchwald and Adams, 1968); (3f) is replaced by

$$D(x) = (1 - e^{\alpha x}) / (1 - e^{\alpha}), \tag{13}$$

from which

$$X(z) = \alpha^{-1} \ln[1 + (1 - e^{\alpha})z]. \tag{14}$$

Using (13) and the surface-intensified stratification (3g) in (5), the critical stratification parameter for this topography is

$$S^c = \begin{cases} (e^{\alpha} - 1) / \alpha, & \text{if } \alpha < \ln(1 + \beta/2), \\ \frac{\beta}{2\alpha} \exp\left(1 - \frac{\beta/2}{e^{\alpha} - 1}\right), & \text{if } \ln(1 + \beta/2) < \alpha < \ln[2/(2 - \beta)], \\ e^{\beta/2}(1 - e^{-\alpha}) / \alpha, & \text{if } \alpha > \ln[2/(2 - \beta)]. \end{cases} \tag{15a}$$

$$\tag{15b}$$

$$\tag{15c}$$

The expressions in (15) correspond to the maximum of (nD_x) occurring: (15a) at $z = 0$, (15b) between z

$= 0$ and $z = -1$, and (15c) at $z = -1$. Fig. 11 shows S^c plotted versus α for various stratifications. The

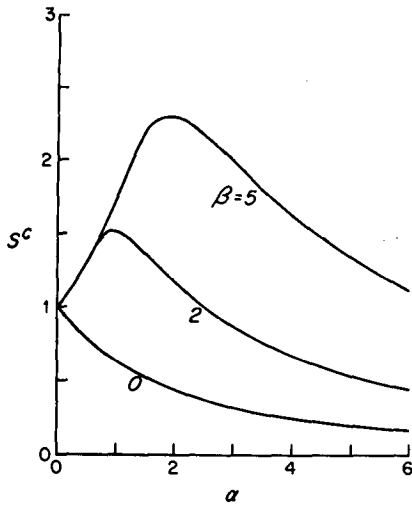


FIG. 11. Critical stratification parameter S^c versus α given by (15) for the exponential topography of (13) and $\beta = 0, 2, 5$.

finite-wedge shelf corresponds to $\alpha \rightarrow 0$. As α increases, making the shelf gentler and the slope steeper, S^c generally decreases in response to the steeper topography. Real coastlines have typical values of $\alpha \approx 4$ or 5 again suggesting that even relatively weak stratification may result in free CTW's with dispersion curves which go to f .

In addition, the mode-1 phase speed at the inertial frequency c_f has been calculated for the uniformly stratified case using (14) and the numerical shooting procedure described in Section 5. Fig. 12 shows c_f plotted versus α . The dashed part of each curve is where c_f is less than the phase speed of the corresponding flat-bottom, baroclinic Kelvin wave, $c_K = S/\pi$. The solid part is where $c_f > c_K$. When S

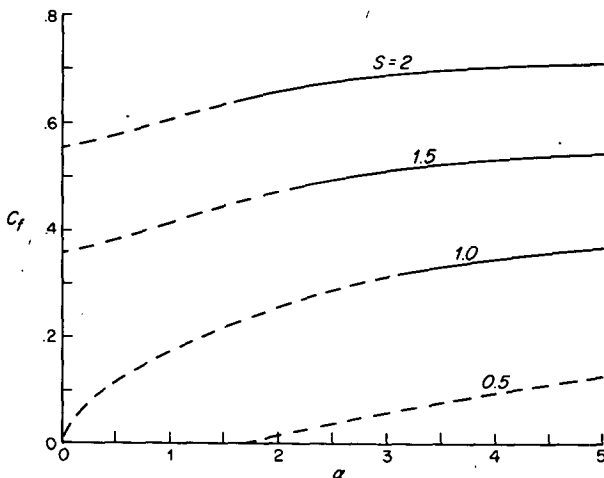


FIG. 12. Scaled, mode-1 phase speed at the inertial frequency c_f versus α for the exponential topography of (13) and $\beta = 0$. Dashed and solid parts of each new curve have the same meaning as in Fig. 5.

is large ($S \geq 2$), c_f is always close to c_K indicating the importance of stratification. Furthermore, if $\alpha \geq 3$, then $c_f > c_K$ for all but the smallest S , again indicating that weak stratification may be important over realistic topography. These qualitative results are unchanged when $\beta > 0$.

Another way of characterizing the importance of stratification is to compare the long-wave and near-inertial results to determine the amount of dispersion in a particular dispersion curve. A "non-dispersion ratio" may be defined as the phase speed at the inertial frequency divided by the long-wave phase speed, $R = c_f/c$, which essentially represents the straightness of the dispersion curve. Each wavenumber-limited dispersion curve has a value between $R = 0$ (the dispersion curve asymptotes to f ; $c_f = 0$) and $R = 1$ (baroclinic Kelvin wave; $c_f = c$). Fig. 13 shows a plot of R versus shelf width L_s for some cases previously considered in Figs. 5 and 9; $\alpha^* = 0.1$, $\beta = 0$. Not surprisingly, the waves are less dispersive (larger R) at larger stratifications. When S is small, the non-dispersion ratio R also increases with shelf width. Also, notice that R is fairly large when $S \geq 1.5$ suggesting that S need not be very large to obtain nearly non-dispersive, baroclinic-Kelvin-like waves with uniform stratification. Strongly surface-intensified stratification substantially reduces the non-dispersion ratio for all (S, L_s) pairs (e.g., $R \approx 0.5$ when $S = 1.5$, $\beta = 5$).

The principal results presented here, while strictly applicable only to the idealized two-slope topography, may also be used to assess the importance of stratification in the modelling of CTW's along real coastlines. A simple test of the importance of stratification (using unscaled variables) can be made by first smoothing the observed profile of the squared buoyancy frequency and fitting it to the function $N^2 \exp(\beta z/H)$. The effect of removing the fine structure on the model predictions has been shown to be negligible (Huthnance, 1978). To obtain a conservative estimate of the importance of stratification, a fit should be made which primarily matches the deep

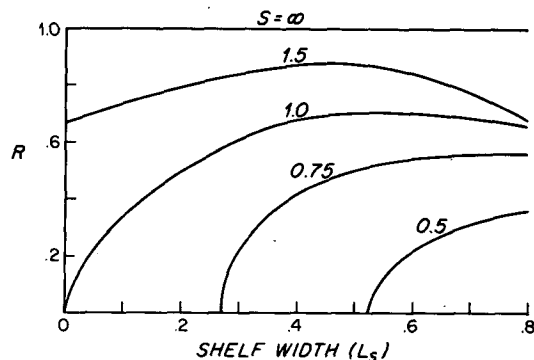


FIG. 13. Non-dispersion ratio $R = c_f/c$ versus shelf width L_s , with $\alpha^* = 0.1$, $\beta = 0$ and $S = 0.5, 0.75, 1.0, 1.5, \infty$.

and mid-depth profiles while ignoring large spikes near the surface. (Large spikes in n^2 will undoubtedly alter the results of Sections 4 and 5. However, if the spikes occur over a gently-sloping shelf, then their effects should not be dominant.) Using the resulting surface value of N , the parameter $(N/f)a_2$ is then calculated, where a_2 is the average bottom slope of the continental slope. A larger $(N/f)a_2$ corresponds to a greater influence of stratification. If $(N/f)a_2 > e^{\beta h/2H}$ where h is the shelf-break depth, then all dispersion curves should go to f . If, in addition, $(N/f)a_2 \geq 3$ and the shelf-break depth is relatively small compared to the deep-ocean depth ($h < 0.2 H$), then the dispersion curves should reach f at relatively small wavenumbers, and stratification effects may be crucial to the accurate modelling of CTW's. This is especially true when the details of the dispersion curves at moderate to large wavenumbers are important (e.g., scattering or resonant interaction problems). For these cases, barotropic models may predict *qualitatively* incorrect behavior. If $(N/f)a_2 < e^{\beta h/2H}$, then the dispersion curves should be limited to frequencies below a sub-inertial maximum. The dispersion curves should look more like the barotropic model predictions, but they will still differ significantly at large wavenumbers. (Note that these results are virtually independent of the shelf slope.)

8. Summary

It should be restated that this paper is not intended to be a comprehensive treatment of CTW's in a continuously stratified ocean. Many simplifications have been made, and the generalizations are based on a limited set of calculations. Nevertheless, the following features of the calculations are sufficiently interesting to be emphasized here.

1) The continental slope and the stratification there primarily determine whether or not the CTW dispersion curves go to f . For fairly realistic topographies and stratifications, if $(N/f)a_2 \geq 1$ then all of the CTW dispersion curves should go to f . If $(N/f)a_2 \leq 1$, then no CTW dispersion curves should reach f . If $(N/f)a_2 \geq 3$, then the mode-1 wave should travel faster than the corresponding flat-bottom, baroclinic Kelvin wave at the inertial frequency.

2) Seemingly weak stratification ($S < 1$) may still be sufficient to cause the CTW dispersion curves to go to f . And even though the deep stratification may be extremely weak, the dispersion curves may still go to f .

3) If the stratification parameter S is greater than unity, then the dispersion curves should generally go to f . With uniform stratification, if $S \geq 1.5$, then the waves should be nearly non-dispersive, baroclinic-Kelvin-like waves.

4) The agreement between predicted long-wave phase speeds in the barotropic and stratified models

generally improves as the shelf width increases (even if S remains fixed) and/or as S decreases.

Acknowledgments. Dr. Allan Clarke contributed much to the analysis shown in the Appendix and to the overall improvement of this work. Dr. Kenneth Brink provided numerous valuable suggestions as well as several computer programs used here. Discussions with Dr. Robert Beardsley and comments from an anonymous reviewer are also gratefully acknowledged. This research was supported by a post-doctoral fellowship from the Woods Hole Oceanographic Institution and by the National Science Foundation under Grants OCE 82-00126 and OCE 80-14941.

APPENDIX

Near-Inertial Solutions for Uniform Stratification

Analytic solutions of (9b,c) may be obtained for the case of the two-slope topography with uniform stratification ($\beta = 0$) by solving for P_0 in the shelf region (upper) and the slope region (lower) individually and then requiring P_0 and dP_0/dz to be continuous at $z = -h$. Using Eq. (10), the upper and lower solutions of (9b) which satisfy (9c) can be written

$$P_0^U = A e^{i\phi_1 z} \left[\cos(l\phi_2 z) - \frac{\phi_1}{\phi_2} \sin(l\phi_2 z) \right], \quad (A1)$$

$$P_0^L = B e^{i\theta_1(z+1)} \left\{ \cos[l\theta_2(z+1)] - \frac{\theta_1}{\theta_2} \sin[l\theta_2(z+1)] \right\}, \quad (A2)$$

where

$$\phi_1 = -1/a_1^*, \quad \phi_2 = [S^2 - (1/a_1^*)^2]^{1/2},$$

$$\theta_1 = -1/a_2^*, \quad \theta_2 = [S^2 - (1/a_2^*)^2]^{1/2}.$$

These pressures must satisfy

$$\left. \begin{aligned} P_0^U &= P_0^L \\ dP_0^U/dz &= dP_0^L/dz \quad \text{at } z = -h \end{aligned} \right\}. \quad (A3)$$

Substitution of (A1) and (A2) into (A3) yields, after some algebraic manipulation,

$$\frac{\phi_2}{\tan(l\phi_2 h)} + \frac{\theta_2}{\tan[l\theta_2(1-h)]} = \theta_1 - \phi_1. \quad (A4)$$

For specified a_1^* , a_2^* and l , the solutions S_m of (A4) are the eigenvalues of (9b,c).

To compare with (6), the critical stratification parameter S^c may be calculated as the limit of S_m as $l \rightarrow \infty$. Because of the square roots in ϕ_2 and θ_2 , it is convenient to consider four ranges of S , letting $l \rightarrow \infty$ in each range.

(i) $S < 1/a_1^*$, $1/a_2^*$. The limit of (A4) as $l \rightarrow \infty$ is

$$|\phi_2| + |\theta_2| = \theta_1 - \phi_1, \quad (A5)$$

for which there are no solutions with $S < 1/a_1^*$, $1/a_2^*$. Thus, for S in this range, no dispersion curves reach $\omega = 1$ for any l .

(ii) $S > 1/a_1^*$, $1/a_2^*$. Eq. (A4) does not simplify as $l \rightarrow \infty$. The left-hand side oscillates at an ever higher frequency, but the right-hand side is a constant. The only possible solutions occur if $\phi_2 = \theta_2 = 0$, but this does not satisfy $S > 1/a_1^*$, $1/a_2^*$. Thus, for S in this range, all dispersion curves reach $\omega = 1$ at finite l .

(iii) $1/a_1^* < S < 1/a_2^*$. As l becomes large, (A4) simplifies to

$$\frac{\phi_2}{\tan(l\phi_2 h)} = \theta_1 - \phi_1 - |\theta_2|. \quad (\text{A6})$$

As l gets ever larger, all solutions coalesce to $\phi_2 \rightarrow 0$ or $S^c \rightarrow 1/a_1^*$.

(iv) $1/a_2^* < S < 1/a_1^*$. This is similar to range (iii) in that (A4) simplifies to

$$\frac{\theta_2}{\tan[l\theta_2(1-h)]} = \theta_1 - \phi_1 - |\phi_2| \quad (\text{A7})$$

for which solutions (as $l \rightarrow \infty$) exist only if $\theta_2 \rightarrow 0$ or $S^c \rightarrow 1/a_2^*$.

These results are consistent with (6) when $\beta = 0$.

REFERENCES

- Brink, K. H., 1982: A comparison of long coastal trapped wave theory with observations off Peru. *J. Phys. Oceanogr.*, **12**, 897-913.
- Buchwald, V. T., and J. K. Adams, 1968: The propagation of continental shelf waves. *Proc. Roy. Soc. London*, **A305**, 235-250.
- Chapman, D. C., 1982: On the failure of Laplace's tidal equations to model subinertial motions at a discontinuity in depth. *Dyn. Atmos. Oceans*, **7**, 1-16.
- , and M. C. Hendershott, 1982: Shelf wave dispersion in a geophysical ocean. *Dyn. Atmos. Oceans*, **7**, 17-31.
- Clarke, A. J., 1976: Coastal upwelling and coastally trapped long waves. Ph.D. dissertation, Cambridge University, 178 pp.
- Huthnance, J. M., 1978: On coastal trapped waves: Analysis and numerical calculation by inverse iteration. *J. Phys. Oceanogr.*, **8**, 74-92.
- Rhines, P., 1970: Edge-, bottom-, and Rossby waves in a rotating stratified fluid. *Geophys. Fluid Dyn.*, **1**, 273-302.
- Romea, R. D., 1982: On coastal-trapped waves at low latitudes in a stratified ocean. Ph.D. dissertation, Oregon State University, 253 pp.